Science of the Total Environment 839 (2022) 156223

Contents lists available at ScienceDirect

Science of the Total Environment

journal homepage: www.elsevier.com/locate/scitotenv

Contamination, sources and health risks of toxic elements in soils of karstic urban parks based on Monte Carlo simulation combined with a receptor model

Zhenjie Zhao [a,b], Ming Hao [c], Yunlong Li [d], Shehong Li [b,*]

[a] Key Laboratory of Environmental Pollution Monitoring and Disease Control, Ministry of Education, School of Public Health, Guizhou Medical University, Guiyang 550025, China
[b] State Key Laboratory of Environmental Geochemistry, Institute of Geochemistry, Chinese Academy of Sciences, Guiyang 550081, China
[c] College of Medical humanities, Guizhou Medical University, Guiyang 550025, China
[d] Shandong Institute of Geophysical and Geochemical Exploration, Jinan 250013, China

HIGHLIGHTS

- Hg and Cd posed highest ecological risks in the study area.
- Four sources governing toxic element contamination were identified.
- The health risk to children was higher than adults.
- Arsenic from coal combustion was the main contributor to the human health risks.

GRAPHICAL ABSTRACT

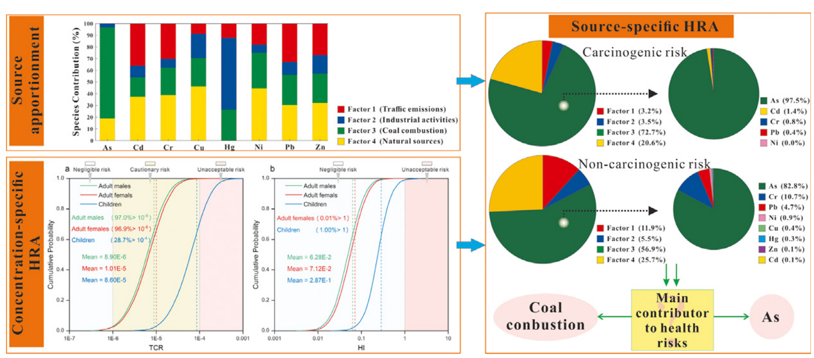

ARTICLE INFO

Editor: Jay Gan

Keywords:
Monte Carlo simulation
Source apportionment
Urban parks
Soil contamination
Heavy metal

ABSTRACT

Understanding the health risks of toxic elements (TEs) in urban park soils and determining their priority control factors are crucial for public health and pollution management. Soil samples were collected from 33 urban parks in Guiyang, a typical karstic city. For each park, 15–45 topsoil samples were collected according to the area and then thoroughly mixed to obtain a representative sample. The results showed that the mean concentrations of TEs in park soils (22.5, 0.37, 88.6, 43.7, 0.26, 39.9, 44.7, and 101.0 mg/kg for As, Cd, Cr, Cu, Hg, Ni, Pb, and Zn, respectively) were higher than their background values. Approximately 54.5% and 33.3% of enrichment factor (EF) values reached moderately enriched to significantly enriched levels for Cd and Hg, respectively. Moreover, 54.5% and 42.4% of monomial potential ecological index (EI) values were at considerable to high risk levels for Cd and Hg, respectively. These results illustrate that Cd and Hg pose high ecological risks. According to the potential ecological risk index (RI) values, 21.2% of the parks were exposed to considerable ecological risk and 48.5% were at moderate risk. Based on the positive matrix factorization (PMF) model, four sources governing TE contamination (including coal combustion, natural sources, traffic emissions, and industrial activities) were identified, with contribution rates of 32.3%, 31.0%, 19.6%, and 17.1%, respectively. A probabilistic health risk assessment showed acceptable non-carcinogenic risks and high levels of carcinogenic risk in all populations. Based on the source-specific health risk assessment, arsenic from coal

Abbreviations: TEs, toxic elements; PMF, positive matrix factorization; HRA, health risk assessment; MCS, Monte Carlo simulation; EF, enrichment factor; RI, potential ecological risk index; EI, monomial potential ecological index; NCR, non-carcinogenic risk; CR, carcinogenic risk; TCR, total carcinogenic risk index; HQ, hazard quotient; HI, hazard index; ADD, average daily intake dose; BV, background values; GV, guide value; CV, coefficients of variation.

* Corresponding author.
E-mail address: lishehong@vip.gyig.ac.cn (S. Li).

http://dx.doi.org/10.1016/j.scitotenv.2022.156223
Received 11 February 2022; Received in revised form 20 May 2022; Accepted 21 May 2022
Available online 25 May 2022

combustion was determined to be a major contributor to human health risks. Although several efforts have been made by the local government to eliminate coal-borne arsenicosis, our results revealed that the accumulation of arsenic in the soil due to coal combustion poses a potential threat to human health.

1. Introduction

Toxic elements (TEs) in urban park soils have a profound effect on human health. Owing to their pronounced cytotoxicity, persistence, insidiousness, and bio-accumulation, TE contamination has raised widespread concern (Han et al., 2021b; Tang et al., 2020; Xiong et al., 2017; Zeng et al., 2022a; Zhao et al., 2022). With rapid industrialization and urbanization, large amounts of TE contaminants have been released into the environment, and urban soils are considered the most prominent ultimate sinks for these TEs (Hiller et al., 2017; Wang et al., 2019b). In China, urban parks are vital recreational spaces for urban dwellers to enjoy outdoor activities, because most residents live in high-rise buildings (Qu et al., 2020; Zhao et al., 2020a). Local residents and frequent visitors to parks are susceptible to exposure to TEs in soil through dermal contact, oral ingestion, or inhalation (Hiller et al., 2017; Huang et al., 2021; Luo et al., 2012). Therefore, understanding the health risks of TEs in urban park soils and determining their priority control factors are critical for public health and pollution management.

To control the risk of TEs in soil to human health, it is necessary to first clarify their source apportionment (Long et al., 2021). Because of the inability to quantify the sources of contaminants, several existing approaches (e.g., cluster analysis, factor analysis, and principal component analysis) are not capable of source-specific risk assessment (Han et al., 2021a). However, the positive matrix factorization (PMF) model developed by U.S. EPA (2014) has been proven to solve this shortcoming by obtaining non-negative results and apportioning the source contribution to each element (Sakizadeh and Zhang, 2021; Song et al., 2021). In this study, geostatistical methods, correlation analysis, and the PMF model were combined to enhance the accuracy of the source apportionment.

The probabilistic health risk assessment (HRA) model provides a reliable means for characterizing the potential human health effects of contaminant exposure. Conventional HRA methods typically rely on deterministic exposure parameter values. However, this may lead to less reliable and informative results because of the inability to avoid uncertainty in HRA (Tong et al., 2018). Instead, Monte Carlo simulation (MCS), a valid probabilistic method, considers the uncertainty and sensitivity of different exposure pathways and thus provides a more realistic risk assessment (Ganyaglo et al., 2019; Kumari and Kumar, 2020). Recently, this probabilistic method has been employed by researchers to examine the potential health risks of contaminants in soils and other aspects of the environment (Huang et al., 2022; Orosun, 2021; Zhang et al., 2021b).

Identifying the main contributors to human health risks is a prerequisite and key step in the prevention and control of soil contamination. Owing to the different contents and toxicity coefficients of TEs, each individual source of contamination can lead to widely varying health risks (Huang et al., 2021; Huang et al., 2018a; Zhao et al., 2020a). Therefore, clarification of the relationship among health risks, TEs, and contamination sources is urgently needed to determine the primary health hazard factors (Sun et al., 2022). However, systematic studies of this relationship are limited. Therefore, this study was conducted to identify the factors that have the greatest impact on human health by elucidating the effects of individual TE and contamination sources on harm risks.

Guizhou Province is located in the center of the world's largest karst region, and includes a unique distribution pattern of soil and water resources and ecological vulnerability (Wang et al., 2020b; Xia et al., 2021). Guizhou contains concentrated energy and mineral resources. Intensified mining activities, rapid urbanization, and industrialization have led to increasingly serious TE contamination in the region (Ma et al., 2020; Ning et al., 2021; Xia et al., 2020). As the capital city of Guizhou Province, Guiyang is the first national forest city and is famous for its good ecological environment and resort tourism. It is also a central industrial city in Southwest China (Tian et al., 2021). Numerous small-scale non-ferrous metal smelters, metal-processing industries, and cement plants exist in the city (Xu et al., 2016). Owing to the rapid growth of vehicles and the limited urban area, traffic in Guiyang is very congested. In addition, Guiyang is rich in coal resources, and coal was extensively used before 2000. However, little attention has been paid to the HRA of soil TE contamination in urban parks in typical karst regions.

Therefore, using Guiyang, a provincial capital city in a karst region as a case study, the present study aimed to: (1) investigate the contamination characteristics of multiple TEs in urban park soils, (2) quantitatively derive their sources, (3) assess the health risks due to exposure to TEs, and (4) determine the major environmental contributors to human health risks in this region.

2. Materials and methods

2.1. Study area and sample collection

Guiyang, the capital city of Guizhou Province, is located in a typical karst area in southwest China. It is a prominent tourism city and has been given the title of 'Summer Capital of China.' At an elevation of 1050 m, the city is controlled by a westerly wind belt year-round. The mean annual temperature of Guiyang is 15.3 °C and the annual precipitation ranges from 1100 to 1400 mm (Tang et al., 2007). Owing to the extensive use of coal, the city has suffered from severe acid rain for many years (Tian et al., 2021). Industry is the backbone of Guiyang's economy, and includes coal-fired power plants, cement, non-ferrous metal smelting and deep processing, tobacco products, pharmaceuticals, and rubber products (Xu et al., 2016). By 2020, the permanent population of Guiyang was 5.99 million, with an urbanization rate of 76%. The urban area of Guiyang covers the districts of Nanming, Yunyan, and several parts of Guanshanhu, Baiyun, Huaxi, and Wudang (Fig. S1).

Samples were collected from 33 parks in the urban area of Guiyang (Fig. S1). Depending on the size of the park and the points at which tourists often gather or pass by, 15–45 sub-samples of topsoil (0–5 cm) were collected from each park (Gu et al., 2016; Huang et al., 2021). The subsamples were then thoroughly mixed with equal weights from each sub sample to obtain a representative sample (Beroigui et al., 2020; Hiller et al., 2017; Liu et al., 2020). The total weight of each composite soil sample was not less than 2 kg. All soils were stored in polyethylene Ziplock bags and transported to the laboratory for further processing.

2.2. Sample preparation and analysis

All soil samples were air-dried at room temperature, ground with an agate mortar, and homogenized through a 100-mesh nylon sieve (0.15 mm) after unnecessary materials, such as plant debris, stones, and gravel, were removed. Ground soil samples were digested with aqua regia. The concentrations of TEs were measured using ICP-MS (NexlON 1000G) and AFS-9750, and the Al content was detected using ICP-OES (Avio 200). Method blanks, duplicates, and the national soil standards (GBW07390, GBW07981, and GBW07404a, respectively) were used to verify the accuracy of the digestion. The recoveries of these elements were 90–110%, and the relative differences among the soil replicates was <5%.

2.3. Soil TE contamination indices

The enrichment factor (EF) was calculated to evaluate the enrichment level and anthropogenic influence on soils as follows (Gujre et al., 2021; Sun et al., 2018):

$$EF = \frac{(C_i/C_x)_{Sample}}{(C_i/C_x)_{Background}} \quad (1)$$

where (C_i/C_x) is the concentration ratio of a particular element (C_i) to the normalized element (C_x) in the soil sample and the reference background. Owing to its large component in soil and immobility, Al is usually chosen as the normalized reference element (Huang et al., 2021; Ma et al., 2020; Tang et al., 2010).

The potential ecological risk index was applied to evaluate the ecological risks of TEs in soil and was calculated as follows:

$$\mathrm{EI} = T_r^i \times \frac{C_i}{S_i} \tag{2}$$

$$\mathrm{RI} = \sum_{i=1}^{n} E_r^i \tag{3}$$

where EI represents the monomial potential ecological index, T_r^i is the toxic response coefficient obtained from Buch et al. (2021). C_i and S_i are the concentrations of each TE in the soil samples and reference background material, respectively. Additionally, n denotes the number of TEs. The evaluation criteria for the EF, EI, and RI are listed in Table S1 (Wu et al., 2021).

2.4. Positive matrix factorization (PMF) model

Receptor models are mathematical techniques that have been extensively adopted in recent years to analyze the contributions of various sources based on sample compositions or fingerprints (Cheng et al., 2020; Wang et al., 2019c). The PMF is a particularly efficient receptor model and a multivariate factor analysis tool recommended by the U.S. EPA for the quantitative apportionment of sources (Huang et al., 2018b; Ran et al., 2021). It offers significant advantages in data preprocessing, including its ability to handle datasets with missing data, analyze data rationality, and estimate uncertainty (Wang et al., 2020a). In this study, EPA PMF 5.0 was applied to obtain potential sources and quantify the contribution from each source to urban park soils. The detailed calculations and explanations of this model are described in the corresponding user guide (U.S. EPA, 2014).

2.5. Health risk assessment (HRA) model

In this study, the HRA model was utilized to calculate the potential health risks (including non-carcinogenic (NCR) and carcinogenic risks (CR)) posed by TEs via different pathways (Adimalla et al., 2020; Men et al., 2021). Considering their behavioral and physiological differences, local residents were classified into three groups: children, adult males, and adult females (Men et al., 2018; Sun et al., 2022). Potential NCR was evaluated based on the hazard quotient (HQ) and hazard index (HI) (Eq. (4)). The potential CR and total carcinogenic risk index (TCR) were quantified using Eq. (5) (Han et al., 2021a; Penteado et al., 2021), as follows:

$$\mathrm{HI} = \sum HQ_i = \sum \frac{ADD_i}{RfD_i} \tag{4}$$

$$\mathrm{TCR} = \sum CR = \sum ADD_{ij} \times SF_{ij} \tag{5}$$

where ADD is the average daily intake dose of TEs via direct ingestion, dermal contact, and inhalation. Detailed calculations of ADD are provided in the Supplementary Materials, and the corresponding indices are provided in Table S2. RfD_i and SF_{ij} are the reference dose and slope factor values, respectively, for each TE (Table S3). Serious non-carcinogenic effects to the public may occur if the HI (or HQ) value is greater than 1; otherwise, the non-carcinogenic effect posed is insignificant (Gu et al., 2016; Gujre et al., 2021). If the TCR (or CR) value exceeds 1×10^{-4}, the carcinogenic risk is unacceptable; if the TCR (or CR) value is less than 1×10^{-6}, there is no apparent risk to human health (Adimalla et al., 2020).

Considering the spatial heterogeneity of TEs in park soil and the inter-individual variability of exposure parameters, HRA results may be subject to high uncertainty or bias (Tarafdar and Sinha, 2018; Tong et al., 2018). To address these shortcomings, a Monte Carlo simulation (MCS, a probabilistic risk approach) was implemented in the HRA model (Gope et al., 2020; Zhang et al., 2021b). The exposure parameters listed in Table S2 were probabilistically simulated. The TE concentrations were also fitted to a lognormal distribution (Table S4). In this study, both concentration- and source-specific health risk assessments were conducted using a MCS in the HRA model.

Table 1
Concentrations of toxic elements (mg/kg) in soils from Guiyang urban parks.

	As	Cd	Cr	Cu	Hg	Ni	Pb	Zn
Mean	22.5	0.37	88.6	43.7	0.26	39.9	44.7	101.0
Median	18.1	0.38	87.2	41.8	0.19	37.5	43.6	100.2
Max.	79.8	0.71	169.0	77.3	0.79	72.3	81.9	206.8
Min.	4.0	0.12	34.1	13.6	0.08	12.8	18.6	41.2
SD	17.8	0.15	28.1	19.5	0.19	17.0	17.8	34.1
CV	0.79	0.41	0.32	0.45	0.73	0.43	0.40	0.34
BV	13.3	0.13	86.6	25.7	0.10	33.7	29.3	82.4
GV	20.0	20.0	n/a	2000.0	8.0	150.0	400.0	n/a
Over BV/%	72.7	97.0	51.5	81.8	93.9	57.6	72.7	72.7

Abbreviations: SD, standard deviation; CV, coefficient of variation; BV, background values for toxic element concentrations in soils in Guizhou Province; GV, guide values of soil environmental quality for development land (GB36600–2018); Over BV, over background value rate.

2.6. Statistical analysis

Descriptive statistics were implemented using SPSS 26. Plots were constructed using GraphPad Prism 8 and Origin 2018. The spatial distributions of the TE content, EF, EI, and RI values were determined using ArcGIS 10.7 with inverse distance weighted interpolation (Zeng et al., 2022b). The MCS was conducted using the Oracle Crystal Ball software, and the simulation was run for 10,000 iterations (Sun et al., 2022; Zhang et al., 2021a).

3. Results and discussion

3.1. Concentrations of toxic elements in soils

The content of most TEs in the soils of the Guiyang urban parks was relatively high. The mean concentrations of TEs ($mg \cdot kg^{-1}$) occurred in the following order: Zn (101.1) > Cr (88.6) > Pb (44.7) > Cu (43.7) > Ni (39.9) > As (22.5) > Cd (0.37) > Hg (0.26) (Table 1). Except for Cr and Ni, the concentrations of the elements were notably higher than their background values (BV) in Guizhou (p < 0.01, one-sample t-test) (Wang and Wei, 1995). In particular, the concentrations of Cd, Hg, Cu, As, and Pb were 2.7-, 2.5-, 1.7-, 1.7, and 1.5 times higher than their BVs, respectively. The

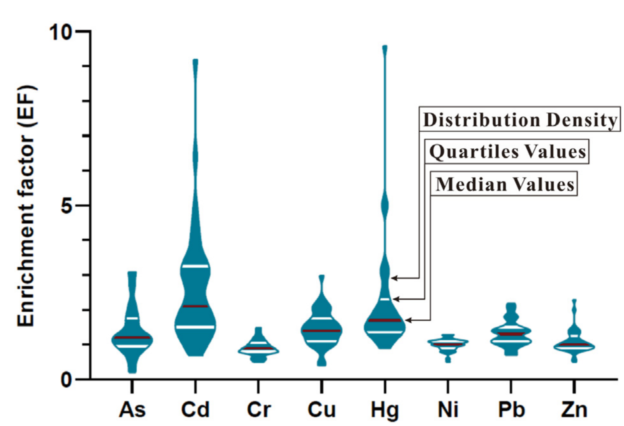

Fig. 1. Violin plots of toxic elements (TEs) with enrichment factor (EF) values in urban park soils of Guiyang.

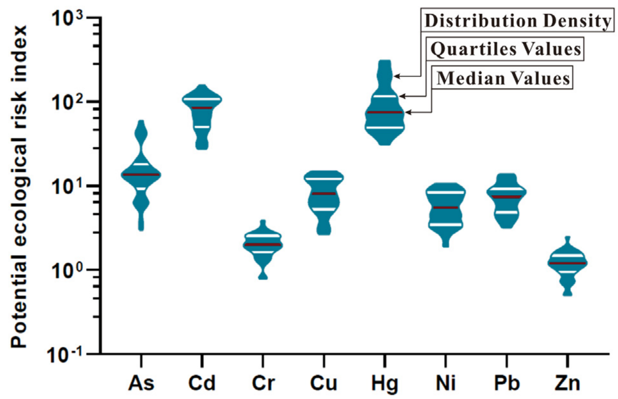

Fig. 2. Violin plots of TEs with monomial potential ecological index (EI) values in urban park soils of Guiyang.

soil concentrations of Cd, Hg, and Cu exceeded their BVs in 97.0%, 93.9%, and 81.8% of the parks, respectively, while the ratios were 72.7% for As, Pb, and Zn. These results indicate that there was a relatively obvious enrichment of elements in addition to Cr and Ni in soils from Guiyang urban parks. Furthermore, the soil As content exceeded the guide value (GV) in 30.3% of the studied parks, suggesting that As may generate potential hazards to the ecological environment and human health.

High heterogeneity was observed in the spatial distributions of elements. All elements had relatively high coefficients of variation (CV > 0.3), especially As and Hg, which had CV values of 0.79 and 0.73, respectively. This suggests that these elements exhibit high spatial variation, and that the distribution of As and Hg might be influenced by external forcing and point sources of contamination (Liu et al., 2021). This result was confirmed by the spatial distribution of the soil element concentrations in the study area (Fig. S2). The spatial distributions of elements can be used to gain insight into the degree of soil contamination and to support the development of remediation methods for managing contaminated soils in the study area (Ran et al., 2021; Zeng et al., 2022b). The spatial patterns and hotspots of Cr, Cu, Ni, Pb, and Zn were highly similar. Moreover, the Pearson correlation coefficients revealed significant positive correlations among most of the TEs in soils, suggesting similar sources or controlling factors (Han et al., 2020; Zeng et al., 2020). Furthermore, all TEs except Cd showed significant positive correlations with Al ($0.52 < r^2 < 0.91, p < 0.01$), indicating a possible influence of soil grain size (Zhao et al., 2021). Overall, the spatial distribution of TEs in park soils differed from west to east, with the element content being higher in the northwest. In addition to the influence of grain size, this pattern may also be related to intensive industrial activity in the northeast. This result is discussed further in Sections 3.2 and 3.3 of this paper.

3.2. Environmental risks of toxic element contamination in soils

Cd and Hg had higher contamination levels than other TEs in the soils. The average EF values of the studied elements decreased in the following order: Cd > Hg > Cu > As > Pb > Zn > Ni > Cr (Fig. 1). Approximately 54.5% and 33.3% of the samples had moderate to significant enrichment levels of Cd and Hg, respectively, which indicated that Cd and Hg occur at relatively high contamination levels. The EF values for Cr and Ni were always below 2, and their mean values were less than 1, indicating that the enrichment of Cr and Ni in park soils was relatively low, which might be influenced by the relatively low level of anthropogenic activity related to these elements compared to that of other elements (Ma et al., 2020). The average EI values of the TEs decreased in the following order: Hg > Cd > As > Cu > Pb > Ni > Cr > Zn (Fig. 2). The average EI values for Hg and Cd were 101.6 and 82.3, respectively, signifying considerable risk. Moreover, approximately 54.5% and 42.4% of the EI values were at considerable to high-risk levels for Cd and Hg, respectively. Therefore, the results of both the EF and EI values illustrated that Cd and Hg pose high ecological risks to the park soils of Guiyang.

Generally, the RI value is related to human activity. The mean RI value for TEs in the study soils was 226.1, indicating a moderate risk. Overall, 21.2% of the parks were exposed to considerable ecological risk and 48.5% were at moderate risk. The spatial variability of the RI value indicated that more seriously contaminated areas occurred in the northwest and central areas of the city (Fig. S3). Dominated by residential and commercial real estate, the central city is the most densely populated, highly visited, and heavily trafficked area (Huang et al., 2021). The northwestern area has the highest concentration of industrial enterprises. The TE contents of park soils in these areas strongly disturbed by anthropogenic activities and were higher in these than in other regions (Liu et al., 2020). Therefore, it is necessary to reinforce the conservation of the soil environments in these regions.

3.3. Source apportionment

Correlation and geographical statistical analyses are effective tools for source apportionment of soil contaminants. As previously noted (Section 3.1), the distribution of TEs in the study area was potentially influenced by soil grain size. Therefore, to eliminate the effect of grain size on TE enrichment, a partial correlation analysis was performed with Al as the control variable (Zhao et al., 2020b; Zhao et al., 2021), and the results are displayed in Fig. 3c. In addition, the EF values for TEs can be used to indicate different sources, including natural or anthropogenic sources (Ma et al., 2020). Geographical statistical analysis, which can be used to visualize the local conditions, is a useful method for identifying contamination hotspots and sources (Huang et al., 2021; Wang et al., 2020c). Hence, spatial variations in the EF values of TEs were determined using GIS methods (Fig. 4).

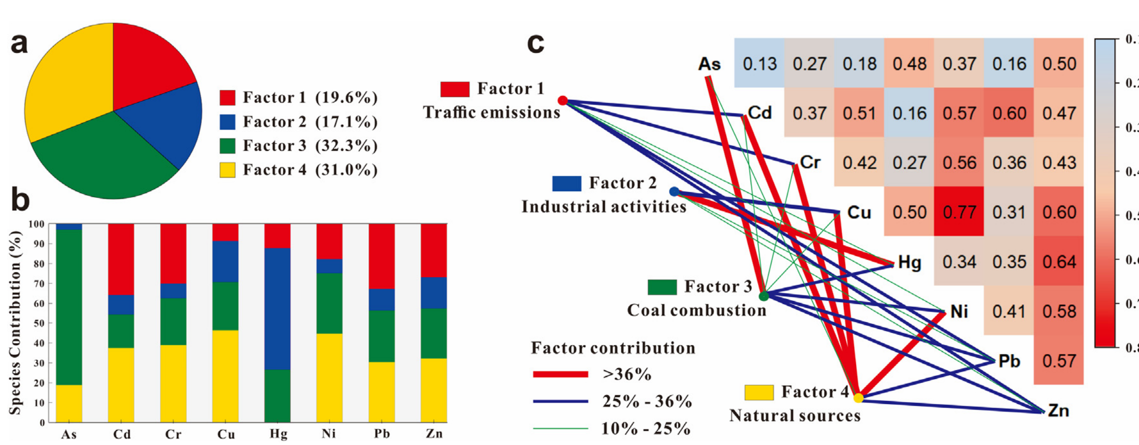

Fig. 3. Source apportionment of TEs in urban park soils of Guiyang. (a) The percentage of different pollution sources. (b) Species contribution of 4 pollution sources for TEs. (c) Combined illustration of 4 sources and partial correlation analysis (Al as the control variable) among TEs.

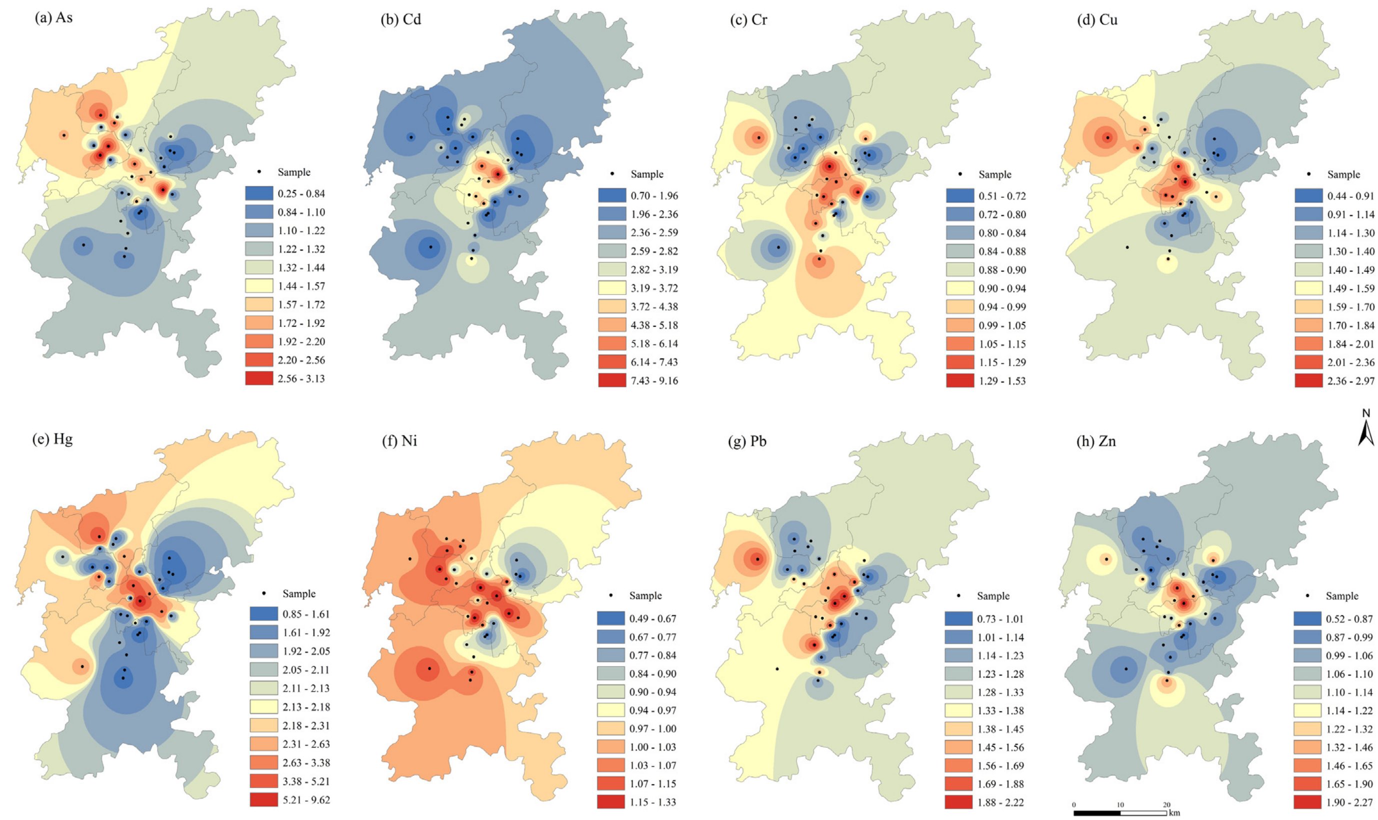

Fig. 4. Spatial variations in enrichment factors of the TEs in urban park soils of Guiyang.

PMF analysis was employed to determine the sources and quantify the contributions of TEs in the Guiyang urban park soils. The number of factors was set from three to five and run 20 times until a minimum and stable Q value was obtained (Ran et al., 2021). Almost all of the residuals were between −3 and 3, and the R^2 values were 0.99, 0.45, 0.73, 0.98, 0.99, 0.95, 0.91, and 0.88 for As, Cd, Cr, Cu, Hg, Ni, Pb, and Zn, suggesting an accurate and rational fit for PMF modeling (Liu et al., 2021; Yang et al., 2020). Consequently, four factors were extracted via the PMF model, with contribution rates of 19.6%, 17.1%, 32.3%, and 31.0%, respectively (Figs. 3 and S4).

Factor 1 may have been associated with traffic emissions. Accounting for 19.6% of the total variance, this factor was characterized by Cd (35.8%), Pb (32.7%), Cr (30.1), and Zn (26.8%) (Figs. 3 and S4). Relatively high correlation coefficients were observed between these elements (Fig. 3c). Moreover, parks with higher EF values were more concentrated in the central city, which has a high traffic volume, according to the GIS map (Fig. 4). Pb and Cd are major markers of a traffic source (Huang et al., 2021). Vehicle emissions are estimated to account for approximately two-thirds of global lead emissions (Fei et al., 2020). Although the use of leaded petrol was prohibited in 2000 in China, considerable levels of Pb still exist in soil due to the centuries-long half-life of Pb (Guan et al., 2018; Wang et al., 2020a). Tire dust, oil burning in automobiles, and braking-related emissions from trains could induce significant non-point Cd contamination in urban areas (Javed et al., 2017; Liang et al., 2017). Zinc is common in automobile tires, lubricant oils, and galvanized parts (Hu et al., 2018; Nazarpour et al., 2019; Thapalia et al., 2015). Hence, the contamination hotspots of Cd, Pb, Cr, and Zn in the central city may be the consequence of traffic emissions.

Factor 2 was allocated to industrial activities such as non-ferrous metal smelting. Accounting for 17.1% of the total variance, this factor had high loading values for Hg (61.2%), followed by Cu (20.7%), and low loadings for Cr (7.3%), Ni (7.0%), and As (2.9%) (Figs. 3 and S4). Mercury, which originates primarily from smelting, coal combustion, and cement production in China, is commonly used to indicate industrial emissions (Fei et al., 2020; Sun et al., 2020). Feng and Qiu (2008) noted that coal combustion and metal smelting were the two main anthropogenic sources of Hg emissions in Guizhou and were responsible for the high Hg content in local ecosystems. Guizhou is a province with abundant coal production and consumption and its coal often contains high levels of arsenic and mercury (Cao et al., 2021). During coal burning, large amounts of contaminants such as As, Cr, and Ni are discharged into the environment, accompanied by the release of mercury (Tian et al., 2014). However, the rather low weight of Cr, Ni, and especially, As, in this factor indicates an industrial source with little impact from coal combustion. In the past few decades, industries such as non-ferrous metal smelting and deep processing, chemical plants, rubber, cement, medicine, and tobacco production have been the pillars of the Guiyang economy. Therefore, this factor was considered to reflect industrial activity.

Factor 3 can be interpreted as coal combustion. Accounting for 32.3% of the total variance, this factor was dominated by As (78.3%), Ni (30.5%), Hg (26.6%), Pb (25.9%), Zn (25.2%), Cu (24.3%), Cr (23.8%), and Cd (16.8%) (Figs. 3 and S4). As has been extensively used as a tracer for coal burning (Olise et al., 2019). Coal in China, especially in Guizhou, has high levels of arsenic compared with other regions of the world (Liang et al., 2017). During coal combustion, large amounts of As are released into the air, water, and soil, resulting in serious environmental contamination. Industries, coal-fired power plants, and residential areas in China are estimated to emit 522, 252, and 21 tons of arsenic into the atmosphere each year, respectively (Kang et al., 2011). Tian et al. (2014), Tian et al., 2011) reported that approximately 550 and 335 t of As were emitted from coal-fired power plants in China in 2007 and 2010, respectively. In addition, numerous studies have demonstrated that many hazardous elements, such as Ni, Hg, Pb, Cr, and Cu, are released during coal combustion (Fei et al., 2020; Wang et al., 2020a). As a large coal-fired city, there are three main combustion systems for coal in Guiyang: large-scale coal-fired power plants (34% of the annual coal supply), medium-to-small-sized coal-fired steam boilers (44% of the annual coal supply), and domestic users (22% of the annual coal supply) (Tang et al., 2007). Emissions of As, Ni, Hg, Pb, Cr, and Cd from coal-fired power plants were estimated to be 8.52, 12.39, 5.2, 13.54, 9.51, and 0.43 t, respectively, in 2010 in Guizhou Province (Tian et al., 2014). The GIS map of EF values confirmed that the hotspots of As were clustered in the central and northwest

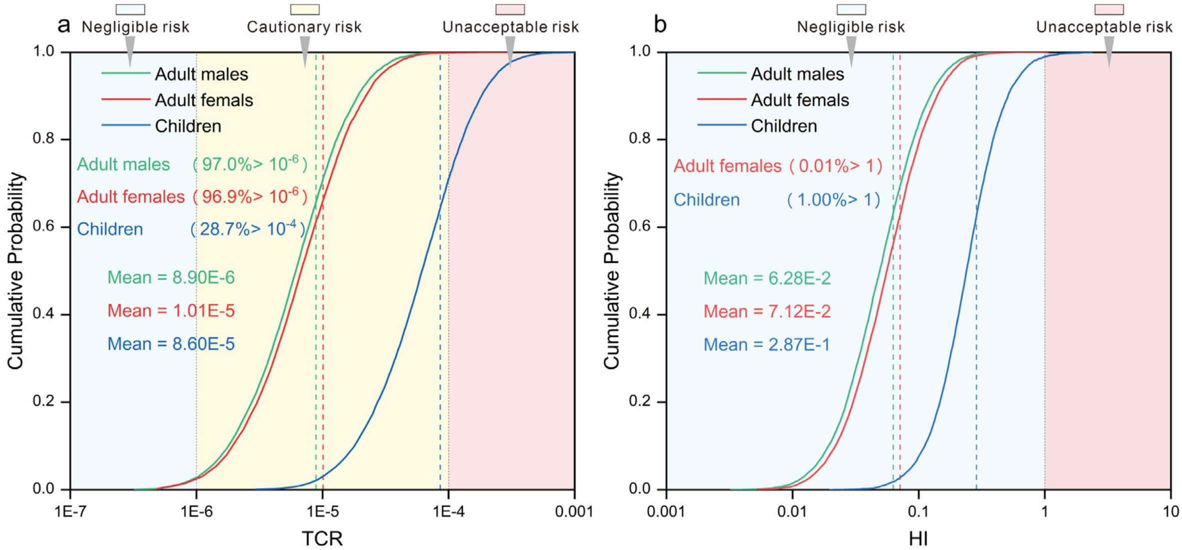

Fig. 5. Cumulative probabilistic estimate of total carcinogenic risk (a) and hazard index (b). The vertical dashed lines in different colors denote the mean values of the different populations.

parts of the city, which have a high density of residents or industrial facilities (Fig. 4). Therefore, this factor was identified as coal combustion.

Factor 4 may be related to natural sources. Accounting for 31.0% of the total variance, this factor was defined as Cu (46.4%), Ni (44.7%), Cr (38.9%), and Cd (37.5%) (Figs. 3 and S4). Relatively high correlation coefficients were found between these elements (Fig. 3c). The mean Cr and Ni concentrations were similar to their local background values (Table 1). The EF values of Cr and Ni in all parks studied were lower than 2, indicating minimal enrichment (Fig. 1). Moreover, the CV values of Cr were lower than those of the other TEs (Table 1) and the EF values of Ni showed a relatively

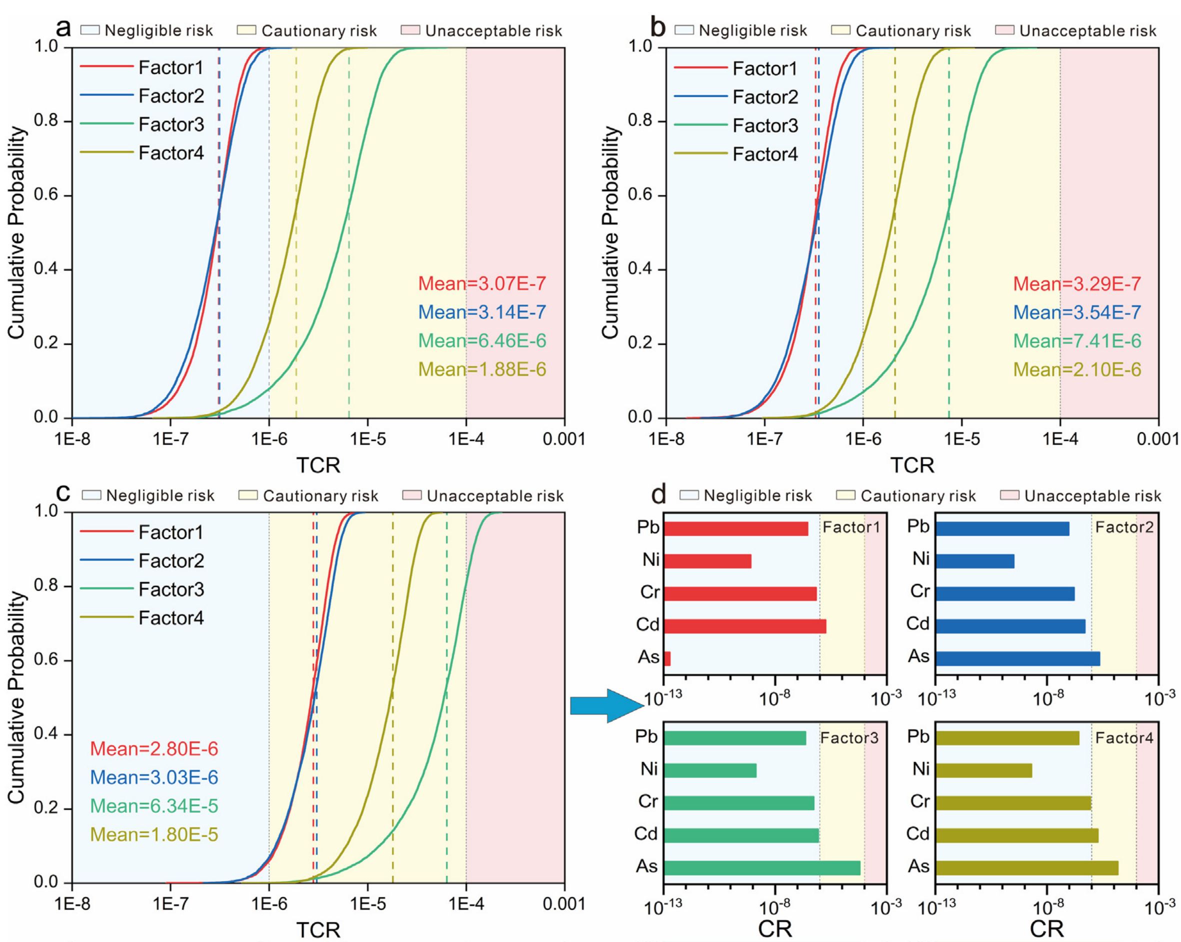

Fig. 6. Cumulative probabilistic estimate of total carcinogenic risk for adult males (a), adult females (b), and children (c) based on source apportionment. (d) The carcinogenic risk of each TE for children according to different sources.

uniform distribution in the GIS map (Fig. 4). These results suggest that Cr and Ni mainly originate from natural sources, with little impact from anthropogenic activities. In fact, Cr and Ni generally have been regarded as indicators of lithologic origin because of their wide presence in soil parent materials (Liu et al., 2021). Therefore, Factor 4 was allocated to geogenic sources such as rock weathering and pedogenic processes.

3.4. Health risks assessment

3.4.1. Concentration-specific HRA

All the populations exhibited high levels of CR. The average TCR values for adult males, females, and children were 8.90E-6, 1.01E-5, and 8.60E-5, respectively (Fig. 5a). Meanwhile, TCR values of approximately 97.0% (adult males), 96.9% (adult females), and 100.0% (children) were higher than the acceptable threshold of 1.0E-6. Additionally, nearly 28.7% of the TCR values exceeded the severe risk level of 1.0E-4 for children. These results suggest a high risk of cancer. Among these elements, As exhibited the highest potential carcinogenic risk to all the populations (Fig. S5). Approximately 88.3% (adult males), 87.7% (adult females), and 100.0% (children) of CR values for As were greater than 1.0E-6. In particular, nearly 25.5% of the CR values for As surpassed 1.0E-4 in children.

NCR for all the populations was negligible. The average HI values for adult males, females, and children were 6.28E-2, 7.12E-2, and 2.87E-1, respectively (Fig. 5b). Similar to the carcinogenic risk results, children suffered from a higher NCR than adults. Moreover, only 1.00% (children) and 0.01% (adult females) of the HI values exceeded the threshold of 1. These results suggest that NCR of these TEs barely threatens human health. The mean HQ values of individual TEs for children decreased as follows: As > Cr > Pb > Ni > Cu > Hg > Cd > Zn, whereas for adults, it decreased as follows: Cr > As > Pb > Cd > Ni > Hg > Cu > Zn (Fig. S6).

3.4.2. Source-specific HRA

The HRA model provided risk levels of contaminants but failed to analyze the contribution of each source to health risk. To compensate for this deficiency, an integrated method was developed by combining the PMF and HRA models (Huang et al., 2021). The results are displayed in Figs. 6-8.

Coal combustion was the dominant source of CR. The change in CR caused by different sources was consistent among different populations, with mean values decreasing as follows: coal combustion source > natural sources > industrial activities > traffic emissions (Fig. 6). For children, the mean CR value of the coal combustion source was 6.34E-5, which was approximately 63 times higher than 1E-6 (the acceptable threshold). Meanwhile, the contribution rates of the four contamination sources to CR decreased in the following order: coal combustion sources (72.7%) > natural sources (20.6%) > industrial activities (3.5%) > traffic emissions (3.2%) (Fig. 8). For specific elements, As showed the highest contribution rates in Factors 2 to 4, with 74.8%, 97.5%, and 83.0% for Factors 2, 3, and 4, respectively. Although the CR value of Factor 1 was mainly contributed by Cd (65.5%), Cr (24.3%), and Pb (10.2%), their contribution to the TCR values was minimal. These results corroborated the view that the health risks were not only related to the content of TEs, but were also closely correlated with the toxicity factor of TEs (Sun et al., 2022).

Similar to the CR results, the most important source of NCR was coal combustion. The change in HI caused by different sources was consistent among the different populations (Fig. 7). In children, the mean HI values of the different sources were 1.64E-1 (coal combustion source), 7.41E-2

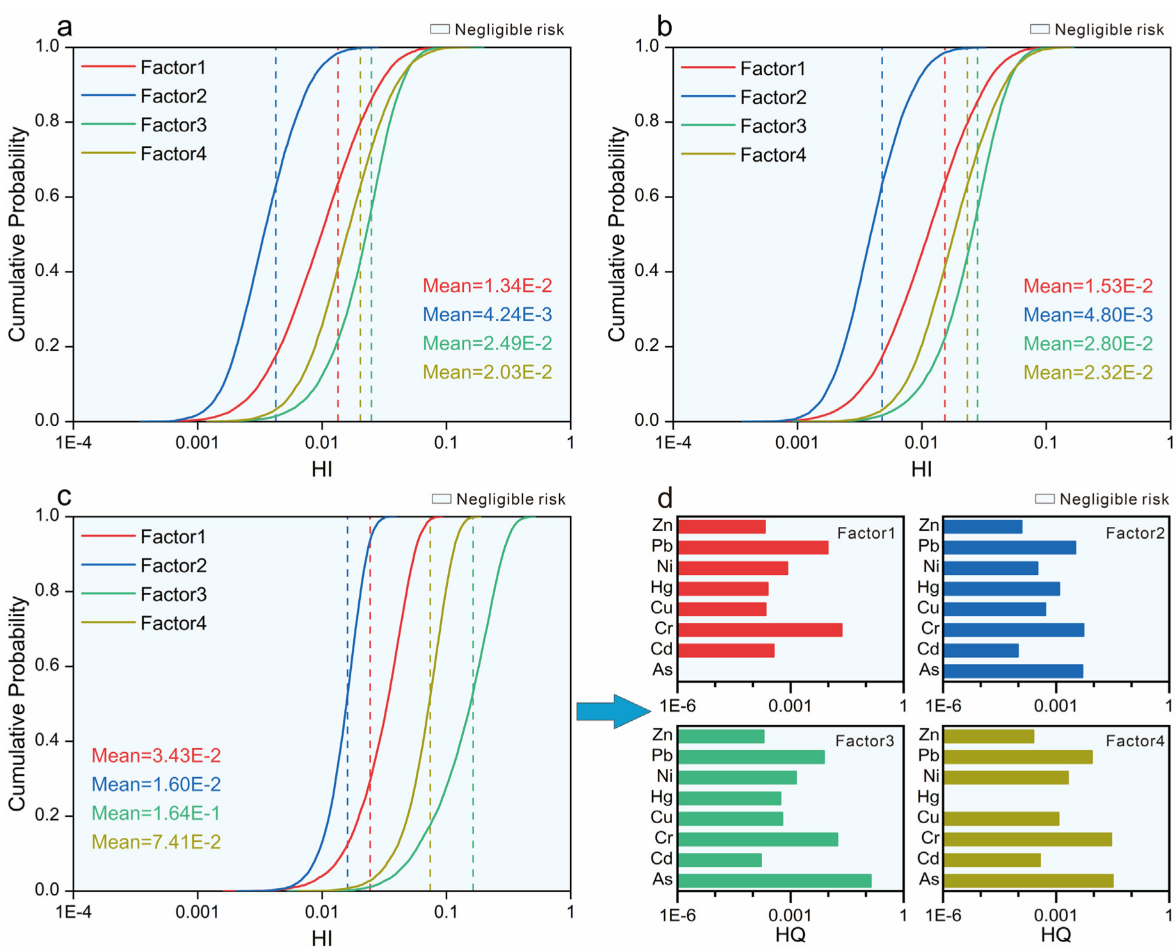

Fig. 7. Cumulative probabilistic estimate of hazard index for adult males (a), adult females (b), and children (c) based on source apportionment. (d) The hazard quotient of each TE for children according to different sources.

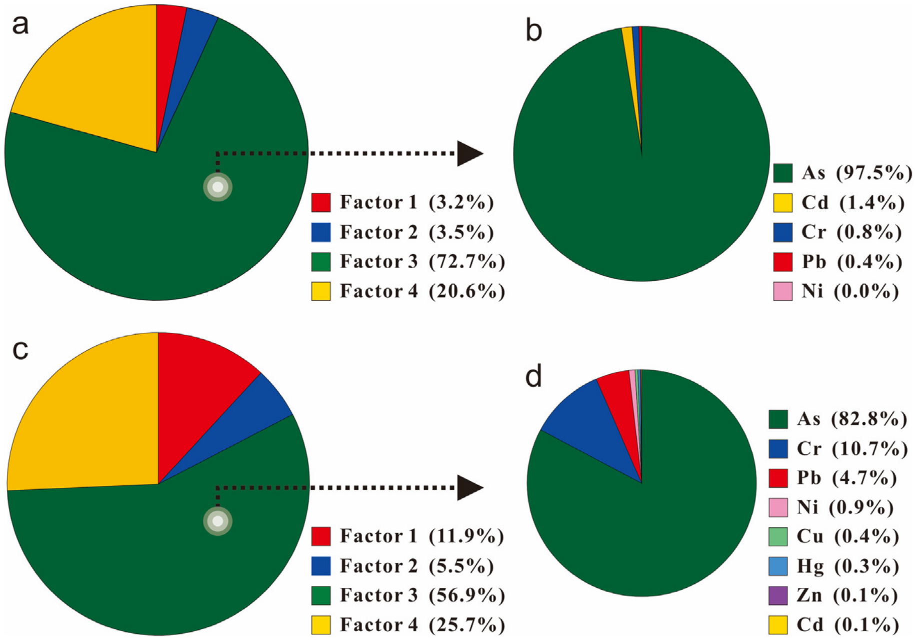

Fig. 8. Contribution percentages of different contamination sources and different TEs to health risk (carcinogenic risk (a and b) and non-carcinogenic risk (c and d)) for children.

(natural sources), 3.43E-2 (traffic emissions), and 1.60E-2 (industrial activities). Meanwhile, the contribution rates of the four sources to NCR decreased in the following order: coal combustion source (56.9%) > natural sources (25.7%) > traffic emissions (11.9%) > industrial activities (5.5%) (Fig. 8). The highest contributions to NCR in the coal combustion and natural sources were made by As, and were 82.8% and 43.3%, respectively. Although Cr and Pb mainly contributed to the HQ values in traffic emissions and industrial activities, they contributed the least to NCR.

Coal combustion was identified as the priority contaminant source and As was identified as the priority contaminant. Overall, coal combustion contributed 72.7% to the carcinogenic risk and 56.9% to the non-carcinogenic risk of TEs in park soils. In the coal combustion source, As played the most important role among the different TEs and caused 97.5% of CR and 82.8% of NCR. Chronical As exposure can lead to a variety of adverse consequences, such as cancer of the liver, skin, lungs, prostate gland, and bladder, as well as coronal heart diseases, polyneuropathy, and black foot disease (Li et al., 2012; Matschullat, 2000). In fact, severe endemic arsenism in Guizhou Province has been detected since 1953 owing to the indoor burning of high-arsenic coal (Zhang et al., 2007; Zheng et al., 2005). Approximately 200,000 residents in the three counties of Guizhou Province are at risk of high As exposure from high-As coal combustion (An et al., 2007). In endemic areas, contaminated indoor air and foods such as corn and chili are considered the main sources of As exposure (Li et al., 2012). Although several efforts have been made by the local government to restrict the mining of high-As coal (Wang et al., 2019a), our results highlight that the accumulation of arsenic in soil due to coal combustion still poses a potential threat to human health.

4. Conclusions

The contamination level, source apportionment, and probabilistic health risk assessment of toxic elements in urban park soils were investigated in a typical karst region in China. The results showed that Hg and Cd were at relatively high contamination levels in most parks. Most TEs exhibited strong spatial heterogeneity owing to the influence of different human activities. Four sources governing TE contamination (coal combustion, natural sources, traffic emissions, and industrial activities) were identified, with contribution percentages of 32%, 31%, 20%, and 17%, respectively. A probabilistic health risk assessment showed acceptable non-carcinogenic risks and high levels of carcinogenic risks in all populations. Based on the source-specific HRA, arsenic from coal combustion was identified as a major contributor to human health risks. Although several efforts have been made by the local government to eliminate coal-borne arsenicosis, our results revealed that the accumulation of arsenic in the soil due to coal combustion poses a great threat to human health.

CRediT authorship contribution statement

Zhenjie Zhao: Conceptualization, Methodology, Resources, Formal analysis, Investigation, Writing - original draft, Writing-review & editing, Visualization, Funding acquisition. **Ming Hao:** Resources. **Yunlong Li:** Investigation. **Shehong Li:** Conceptualization, Supervision, Writing - original draft, Writing-review & editing, Funding acquisition.

Declaration of competing interest

The authors declare that they have no known competing financial interests or personal relationships that could have appeared to influence the work reported in this paper.

Acknowledgements

This work was supported by the United Fund of the Guizhou Province Government and Natural Science Foundation of China (No. U1612442), Guizhou Provincial Science and Technology Projects (ZK[2022]405), Opening Fund of the State Key Laboratory of Environmental Geochemistry (SKLEG2022215), and Guizhou Medical University with High Level Talents Project (XBHJZ[2021]012).

Appendix A. Supplementary data

Supplementary data to this article can be found online at https://doi.org/10.1016/j.scitotenv.2022.156223.

References

Adimalla, N., Chen, J., Qian, H., 2020. Spatial characteristics of heavy metal contamination and potential human health risk assessment of urban soils: a case study from an urban region of South India. Ecotoxicol. Environ. Saf. 194, 110406.

An, D., Li, D., Liang, Y., Jing, Z., 2007. Unventilated indoor coal-fired stoves in Guizhou Province, China: reduction of arsenic exposure through behavior changes resulting from mitigation and health education in populations with arsenicosis. Environ. Health Perspect. 115, 659–662.

Beroigui, M., et al., 2020. Physicochemical and microbial properties of urban park soils of the cities of Marrakech, Morocco and Torun, Poland: human health risk assessment of fecal coliforms and trace elements. Catena 194, 104673.

Buch, A.C., Niemeyer, J.C., Marques, E.D., Silva, E.V., 2021. Ecological risk assessment of trace metals in soils affected by mine tailings. J. Hazard. Mater. 403, 123852.

Cao, Q., Yang, L., Ren, W., Song, Y., Huang, S., Wang, Y., Wang, Z., 2021. Spatial distribution of harmful trace elements in chinese coalfields: an application of WebGIS technology. Sci. Total Environ. 755, 142527.

Cheng, W., Lei, S.G., Bian, Z.F., Zhao, Y.B., Li, Y.C., Gan, Y.D., 2020. Geographic distribution of heavy metals and identification of their sources in soils near large, open-pit coal mines using positive matrix factorization. J. Hazard. Mater. 387, 121666.

Fei, X.F., Lou, Z.H., Xiao, R., Ren, Z.Q., Lv, X.N., 2020. Contamination assessment and source apportionment of heavy metals in agricultural soil through the synthesis of PMF and GeogDetector models. Sci. Total Environ. 747, 141293.

Feng, X.B., Qiu, G.L., 2008. Mercury pollution in Guizhou, southwestern China - an overview. Sci. Total Environ. 400, 227–237.

Ganyaglo, S.Y., Gibrilla, A., Teye, E.M., Owusu-Ansah, E.D.-G.J., Tettey, S., Diabene, P.Y., Asimah, S., 2019. Groundwater fluoride contamination and probabilistic health risk assessment in fluoride endemic areas of the upper east region, Ghana. Chemosphere 233, 862–872.

Gope, M., Masto, R.E., Basu, A., Bhattacharyya, D., Saha, R., Hoque, R.R., Khillare, P.S., Balachandran, S., 2020. Elucidating the distribution and sources of street dust bound PAHs in Durgapur, India: a probabilistic health risk assessment study by Monte-Carlo simulation. Environ. Pollut. 267, 115669.

Gu, Y.G., Lin, Q., Gao, Y.P., 2016. Metals in exposed-lawn soils from 18 urban parks and its human health implications in southern China's largest city, Guangzhou. J. Clean. Prod. 115, 122–129.

Guan, Q.Y., Wang, F.F., Xu, C.Q., Pan, N.H., Lin, J.K., Zhao, R., Yang, Y.Y., Luo, H.P., 2018. Source apportionment of heavy metals in agricultural soil based on PMF: a case study in hexi corridor, Northwest China. Chemosphere 193, 189–197.

Gujre, N., Mitra, S., Soni, A., Agnihotri, R., Rangan, L., Rene, E.R., Sharma, M.P., 2021. Speciation, contamination, ecological and human health risks assessment of heavy metals in soils dumped with municipal solid wastes. Chemosphere 262, 128013.

Han, Q., Wang, M.S., Cao, J.L., Gui, C.L., Liu, Y.P., He, X.D., He, Y.C., Liu, Y., 2020. Health risk assessment and bioaccessibilities of heavy metals for children in soil and dust from urban parks and schools of Jiaozuo, China. Ecotoxicol. Environ. Saf. 191, 110157.

Han, J., Lee, S., Mammadov, Z., Kim, M., Mammadov, G., Ro, H.M., 2021a. Source apportionment and human health risk assessment of trace metals and metalloids in surface soils of the mugan plain, the republic of Azerbaijan. Environ. Pollut. 290, 118058.

Han, Q., Liu, Y., Feng, X.X., Mao, P., Sun, A., Wang, M.Y., Wang, M.S., 2021b. Pollution effect assessment of industrial activities on potentially toxic metal distribution in windowsill dust and surface soil in Central China. Sci. Total Environ. 759, 144023.

Hiller, E., Mihaljevic, M., Filova, L., Lachka, L., Jurkovic, L., Kulikova, T., Fajcikova, K., Simurkova, M., Tatarkova, V., 2017. Occurrence of selected trace metals and their oral bioaccessibility in urban soils of kindergartens and parks in Bratislava (Slovak Republic) as evaluated by simple in vitro digestion procedure. Ecotoxicol. Environ. Saf. 144, 611–621.

Hu, W.Y., Wang, H.F., Dong, L.R., Huang, B.A., Borggaard, O.K., Hansen, H.C.B., He, Y., Holm, P.E., 2018. Source identification of heavy metals in peri-urban agricultural soils of Southeast China: an integrated approach. Environ. Pollut. 237, 650–661.

Huang, R.J., Cheng, R., Jing, M., Yang, L., Li, Y., Chen, Q., Chen, Y., Yan, J., Lin, C., Wu, Y., Zhang, R., El Haddad, I., Prevot, A.S.H., O'Dowd, C.D., Cao, J., 2018a. Source-specific health risk analysis on particulate trace elements: coal combustion and traffic emission as major contributors in wintertime Beijing. Environ. Sci. Technol. 52, 10967–10974.

Huang, Y., Deng, M.H., Wu, S.F., Jan, J.P.G., Li, T.Q., Yang, X.E., He, Z.L., 2018b. A modified receptor model for source apportionment of heavy metal pollution in soil. J. Hazard. Mater. 354, 161–169.

Huang, J.L., Wu, Y.Y., Sun, J.X., Li, X., Geng, X.L., Zhao, M.L., Sun, T., Fan, Z.Q., 2021. Health risk assessment of heavy elements in park soils of the largest megacity in China by using Monte Carlo simulation coupled with positive matrix factorization model. J. Hazard. Mater. 415, 125629.

Huang, S., Li, Q., Liu, H., Ma, S., Long, C., Li, G., Yu, Y., 2022. Urinary monohydroxylated polycyclic aromatic hydrocarbons in the general population from 26 provincial capital cities in China: levels, influencing factors, and health risks. Environ. Int. 160, 107074.

Javed, M.T., Akram, M.S., Tanwir, K., Chaudhary, H.J., Ali, Q., Stoltz, E., Lindberg, S., 2017. Cadmium spiked soil modulates root organic acids exudation and ionic contents of two differentially cd tolerant maize (Zea mays L.) cultivars. Ecotoxicol. Environ. Saf. 141, 216–225.

Kang, Y., Liu, G., Chou, C.-L., Wong, M.H., Zheng, L., Ding, R., 2011. Arsenic in chinese coals: distribution, modes of occurrence, and environmental effects. Sci. Total Environ. 412–413, 1–13.

Kumari, M., Kumar, A., 2020. Human health risk assessment of antibiotics in binary mixtures for finished drinking water. Chemosphere 240, 124864.

Li, S.H., Xiao, T.F., Zheng, B.S., 2012. Medical geology of arsenic, selenium and thallium in China. Sci. Total Environ. 421–422, 31–40.

Liang, J., Feng, C.T., Zeng, G.M., Gao, X., Zhong, M.Z., Li, X.D., Li, X., He, X.Y., Fang, Y.L., 2017. Spatial distribution and source identification of heavy metals in surface soils in a typical coal mine city, Lianyuan, China. Environ. Pollut. 225, 681–690.

Liu, L., Liu, Q., Ma, J., Wu, H., Qu, Y., Gong, Y., Yang, S., An, Y., Zhou, Y., 2020. Heavy elements in the topsoil of urban parks in Beijing, China: concentrations, potential sources, and risk assessment. Environ. Pollut. 260, 114083.

Liu, H.W., Zhang, Y., Yang, J.S., Wang, H.Y., Li, Y.L., Shi, Y., Li, D.C., Holm, P.E., Ou, Q., Hu, W.Y., 2021. Quantitative source apportionment, risk assessment and distribution of heavy metals in agricultural soils from southern Shandong peninsula of China. Sci. Total Environ. 767, 144879.

Long, Z.J., Zhu, H., Bing, H.J., Tian, X., Wang, Z.G., Wang, X.F., Wu, Y.H., 2021. Contamination, sources and health risk of heavy metals in soil and dust from different functional areas in an industrial city of Panzhihua City, Southwest China. J. Hazard. Mater. 420, 126638.

Luo, X.S., Ding, J., Xu, B., Wang, Y.J., Li, H.B., Yu, S., 2012. Incorporating bioaccessibility into human health risk assessments of heavy metals in urban park soils. Sci. Total Environ. 424, 88–96.

Ma, L., Xiao, T.F., Ning, Z.P., Liu, Y.Z., Chen, H.Y., Peng, J.Q., 2020. Pollution and health risk assessment of toxic elements in soils under different land use in sulphide mineralized areas. Sci. Total Environ. 724, 138176.

Matschullat, J., 2000. Arsenic in the geosphere - a review. Sci. Total Environ. 249, 297–312.

Men, C., Liu, R.M., Xu, F., Wang, Q.R., Guo, L.J., Shen, Z.Y., 2018. Pollution characteristics, risk assessment, and source apportionment of heavy metals in road dust in Beijing, China. Sci. Total Environ. 612, 138–147.

Men, C., Liu, R.M., Wang, Q.R., Miao, Y.X., Wang, Y.F., Jiao, L.J., Li, L., Cao, L.P., Shen, Z.Y., Li, Y., Crawford, D., 2021. Spatial-temporal characteristics, source-specific variation and uncertainty analysis of health risks associated with heavy metals in road dust in Beijing, China. Environ. Pollut. 278, 116866.

Nazarpour, A., Watts, M.J., Madhani, A., Elahi, S., 2019. Source, spatial distribution and pollution assessment of pb, zn, cu, and pb, isotopes in urban soils of Ahvaz City, a semi-arid metropolis in Southwest Iran. Sci. Rep. 9, 5349.

Ning, Z., Liu, E., Yao, D., Xiao, T., Ma, L., Liu, Y., Li, H., Liu, C., 2021. Contamination, oral bioaccessibility and human health risk assessment of thallium and other elements in farmland soils around a historic tl hg mining area. Sci. Total Environ. 758, 143577.

Olise, F.S., Ogundele, L.T., Olajire, M.A., Owoade, O.K., Oloyede, F.A., Fawole, O.G., Ezeh, G.C., 2019. Biomonitoring of environmental pollution in the vicinity of iron and steel smelters in southwestern Nigeria using transplanted lichens and mosses. Environ. Monit. Assess. 191, 1–13.

Orosun, M.M., 2021. Assessment of arsenic and its associated health risks due to mining activities in parts of north-Central Nigeria: probabilistic approach using Monte Carlo. J. Hazard. Mater. 412, 125262.

Penteado, J.O., Brum, R.D., Ramires, P.F., Garcia, E.M., dos Santos, M., da Silva, F.M.R., 2021. Health risk assessment in urban parks soils contaminated by metals, Rio Grande City (Brazil) case study. Ecotoxicol. Environ. Saf. 208, 111737.

Qu, Y., Gong, Y., Ma, J., Wei, H., Liu, Q., Liu, L., Wu, H., Yang, S., Chen, Y., 2020. Potential sources, influencing factors, and health risks of polycyclic aromatic hydrocarbons (PAHs) in the surface soil of urban parks in Beijing, China. Environ. Pollut. 260, 114016.

Ran, H.Z., Guo, Z.H., Yi, L.W., Xiao, X.Y., Zhang, L., Hu, Z.H., Li, C.Z., Zhang, Y.X., 2021. Pollution characteristics and source identification of soil elements at an abandoned arsenic-containing mine, China. J. Hazard. Mater. 413, 125382.

Sakizadeh, M., Zhang, C.S., 2021. Source identification and contribution of land uses to the observed values of heavy metals in soil samples of the border between the Northern Ireland and Republic of Ireland by receptor models and redundancy analysis. Geoderma 404, 115313.

Song, Z.C., Wang, C., Ding, L., Chen, M., Hu, Y.X., Li, P., Zhang, L.M., Feng, X.B., 2021. Soil mercury pollution caused by typical anthropogenic sources in China: evidence from stable mercury isotope measurement and receptor model analysis. J. Clean. Prod. 288, 125687.

Sun, X.S., Fan, D.J., Liu, M., Tian, Y., Pang, Y., Liao, H.J., 2018. Source identification, geochemical normalization and influence factors of heavy metals in Yangtze River estuary sediment. Environ. Pollut. 241, 938–949.

Sun, G.Y., Feng, X.B., Yang, C.M., Zhang, L.M., Yin, R.S., Li, Z.G., Bi, X.Y., Wu, Y.J., 2020. Levels, sources, isotope signatures, and health risks of mercury in street dust across China. J. Hazard. Mater. 392, 122276.

Sun, J.X., Zhao, M.L., Huang, J.L., Liu, Y.F., Wu, Y.Y., Cai, B.Y., Han, Z.W., Huang, H.H., Fan, Z.Q., 2022. Determination of priority control factors for the management of soil trace elements based on source-oriented health risk assessment. J. Hazard. Mater. 423, 127116.

Tang, S.L., Feng, X.B., Qiu, H.R., Yin, G.X., Yang, Z.C., 2007. Mercury speciation and emissions from coal combustion in Guiyang, Southwest China. Environ. Res. 105, 175–182.

Tang, W.Z., Shan, B.Q., Zhang, H., Mao, Z.P., 2010. Heavy metal sources and associated risk in response to agricultural intensification in the estuarine sediments of Chaohu Lake Valley, East China. J. Hazard. Mater. 176, 945–951.

Tang, W.Z., Sun, L., Shu, L.M., Wang, C., 2020. Evaluating heavy metal contamination of riverine sediment cores in different land-use areas. Front. Environ. Sci. Eng. 14, 104.

Tarafdar, A., Sinha, A., 2018. Public health risk assessment with bioaccessibility considerations for soil PAHs at oil refinery vicinity areas in India. Sci. Total Environ. 616, 1477–1484.

Thapalia, A., Borrok, D.M., Van Metre, P.C., Wilson, J., 2015. Zinc isotopic signatures in eight lake sediment cores from across the United States. Environ. Sci. Technol. 49, 132–140.

Tian, H., Wang, Y., Xue, Z., Qu, Y., Chai, F., Hao, J., 2011. Atmospheric emissions estimation of hg, as, and se from coal-fired power plants in China, 2007. Sci. Total Environ. 409, 3078–3081.

Tian, H., Liu, K., Zhou, J., Lu, L., Hao, J., Qiu, P., Gao, J., Zhu, C., Wang, K., Hua, S., 2014. Atmospheric emission inventory of hazardous trace elements from China's coal-fired power plants—Temporal trends and spatial variation characteristics. Environ. Sci. Technol. 48, 3575–3582.

Tian, J., Guan, H., Zhou, Y., Zheng, N., Xiao, H., Zhao, J., Zhang, Z., Xiao, H., 2021. Isotopic source analysis of nitrogen-containing aerosol: a study of PM2.5 in Guiyang (SW, China). Sci. Total Environ. 760, 143935.

Tong, R.P., Yang, X.Y., Su, H.R., Pan, Y., Zhang, Q.Z., Wang, J., Long, M.C., 2018. Levels, sources and probabilistic health risks of polycyclic aromatic hydrocarbons in the agricultural soils from sites neighboring suburban industries in Shanghai. Sci. Total Environ. 616, 1365–1373.

U.S. EPA, 2014. EPA Positive Matrix Factorization (PMF) 5.0 Fundamentals and User Guide. U.S. Environmental Protection Agency.

Wang, Y., Wei, F.S., 1995. Elemental Chemistry of Soil Environment. Environmental Science, Beijing (in Chinese).

Wang, D.P., Luo, P., Zou, Z.L., Wang, Q.L., Yao, M.L., Yu, C., Wei, S.F., Sun, B.F., Zhu, K., Zeng, Q.B., Li, J., Liang, B., Zhang, A.H., 2019a. Alterations of arsenic levels in arsenicosis residents and awareness of its risk factors: a population-based 20-year follow-up study in a unique coal-borne arsenicosis county in Guizhou, China. Environ. Int. 129, 18–27.

Wang, M., Han, Q., Gui, C., Cao, J., Liu, Y., He, X., He, Y., 2019b. Differences in the risk assessment of soil heavy metals between newly built and original parks in Jiaozuo, Henan Province, China. Sci. Total Environ. 676, 1–10.

Wang, S., Cai, L.M., Wen, H.H., Luo, J., Wang, Q.S., Liu, X., 2019c. Spatial distribution and source apportionment of heavy metals in soil from a typical county-level city of Guangdong Province, China. Sci. Total Environ. 655, 92–101.

Wang, F.F., Guan, Q.Y., Tian, J., Lin, J.K., Yang, Y.Y., Yang, L.Q., Pan, N.H., 2020a. Contamination characteristics, source apportionment, and health risk assessment of heavy metals in agricultural soil in the hexi corridor. Catena 191, 104573.

Wang, J., Chen, J., Jin, Z., Guo, J., Yang, H., Zeng, Y., Liu, Y., 2020b. Simultaneous removal of phosphate and ammonium nitrogen from agricultural runoff by amending soil in lakeside zone of karst area, southern China. Agric. Ecosyst. Environ. 289, 106745.

Wang, X.Y., Liu, E.F., Lin, Q., Liu, L., Yuan, H.Z., Li, Z.J., 2020d. Occurrence, sources and health risks of toxic elements in road dust from a mega city (Nanjing) in China. Environ. Pollut. 263, 114518.

Wu, Q.M., Hu, W.Y., Wang, H.F., Liu, P., Wang, X.K., Huang, B.A., 2021. Spatial distribution, ecological risk and sources of heavy metals in soils from a typical economic development area, southeastern China. Sci. Total Environ. 780, 146557.

Xia, Y., Gao, T., Liu, Y., Wang, Z., Liu, C., Wu, Q., Qi, M., Lv, Y., Li, F., 2020. Zinc isotope revealing zinc's sources and transport processes in karst region. Sci. Total Environ. 724, 138191.

Xia, J.C., Wang, J.X., Zhang, L.M., Wang, X., Yuan, W., Zhang, H., Peng, T., Feng, X.B., 2021. Mass balance of nine trace elements in two karst catchments in Southwest China. Sci. Total Environ. 786, 147504.

Xiong, Y., Xiao, T.F., Liu, Y.Z., Zhu, J.M., Ning, Z.P., Xiao, Q.X., 2017. Occurrence and mobility of toxic elements in coals from endemic fluorosis areas in the three gorges region, SW China. Ecotoxicol. Environ. Saf. 144, 1–10.

Xu, X.H., Liu, N., Landis, M.S., Feng, X.B., Qiu, G.L., 2016. Characteristics and distributions of atmospheric mercury emitted from anthropogenic sources in Guiyang, southwestern China. Acta Geochimica 35, 240–250.

Yang, S.H., Qu, Y.J., Ma, J., Liu, L.L., Wu, H.W., Liu, Q.Y., Gong, Y.W., Chen, Y.X., Wu, Y.H., 2020. Comparison of the concentrations, sources, and distributions of heavy elements in agricultural soils of two provinces in the Yangtze River Delta, China. Environ. Pollut. 264, 114688.

Zeng, J., Han, G., Yang, K., 2020. Assessment and sources of heavy metals in suspended particulate matter in a tropical catchment, Northeast Thailand. J. Clean. Prod. 265, 121898.

Zeng, J., Han, G., Zhang, S., Liang, B., Qu, R., Liu, M., Liu, J., 2022a. Potentially toxic elements in cascade dams-influenced river originated from tibetan plateau. Environ. Res. 208, 112716.

Zeng, J., Luo, X., Cheng, Y., Ke, W., Hartley, W., Li, C., Jiang, J., Zhu, F., Xue, S., 2022b. Spatial distribution of toxic elements at an abandoned zinc smelting site, southern China. J. Hazard. Mater. 425, 127970.

Zhang, A.H., Feng, H., Yang, G.H., Pan, X.L., Jiang, X.Y., Huang, X.X., Dong, X.X., Yang, D.P., Xie, Y.X., Peng, L., Jun, L., Hu, C., Jian, L., Wang, X.L., 2007. Unventilated indoor coal-fired stoves in Guizhou Province, China: cellular and genetic damage in villagers exposed to arsenic in food and air. Environ. Health Perspect. 115, 653–658.

Zhang, H.W., Zhang, F., Song, J., Tan, M.L., Kung, H.T., Johnson, V.C., 2021a. Pollutant source, ecological and human health risks assessment of heavy metals in soils from coal mining areas in Xinjiang, China. Environ. Res. 202, 111702.

Zhang, Y., Guo, Z.H., Peng, C., Deng, H.Y., Xiao, X.Y., 2021b. A questionnaire based probabilistic risk assessment (PRA) of heavy metals in urban and suburban soils under different land uses and receptor populations. Sci. Total Environ. 793, 148525.

Zhao, L.S., Yan, Y., Yu, R.L., Hu, G.R., Cheng, Y.F., Huang, H.B., 2020a. Source apportionment and health risks of the bioavailable and residual fractions of heavy metals in the park soils in a coastal city of China using a receptor model combined with pb isotopes. Catena 194, 104736.

Zhao, Z.J., Li, S.H., Xue, L.L., Liao, J., Zhao, J.J., Wu, M., Wang, M.G., Sun, J., Zheng, Y., Yang, Q., 2020b. Effects of dam construction on arsenic mobility and transport in two large rivers in Tibet, China. Sci. Total Environ. 741, 140406.

Zhao, Z.J., Li, S.H., Xue, L.L., Liao, J., Zhao, J.J., Wu, M., Wang, M.G., Yang, Q., Sun, J., Zheng, Y., 2021. Abundance and mobility of elements in reservoir sediments of singe tsangpo and yarlung tsangpo in Tibet, China: implications for ecological risk. Environ. Geochem. Health 43, 3213–3228.

Zhao, Z.J., Li, S.H., Wang, S.L., Liao, J., Lu, W.Q., Tan, D., Yang, D., 2022. Heavy metal characteristics in porewater profiles, their benthic fluxes, and toxicity in cascade reservoirs of the Lancang River, China. Environ. Sci. Pollut. Res. https://doi.org/10.1007/s11356-022-18652-x.

Zheng, B.S., Wang, B.B., Ding, Z.H., Zhou, D.X., Zhou, Y.S., Zhou, C., Chen, C.C., Finkelman, R.B., 2005. Endemic arsenosis caused by indoor combustion of high-As coal in Guizhou Province, P.R. China. Environ. Geochem. Health 27, 521–528.